Gazi Üniversitesi
Fen Bilimleri Dergisi
PART C: TASARIM VE TEKNOLOJİ

Gazi University
Journal of Science
PART C: DESIGN AND TECHNOLOGY

GU J Sci, Part C, 13(1): 341-354 (2025)

Analysis of Mechanical and Thermal Material Characteristics of GPL-Reinforced Double-FG Composite Nanoplates under Temperature Load

Kerim Gökhan AKTAŞ[1*]

[1]*Karabuk University, Faculty of Engineering, Department of Mechanical Engineering, Karabuk, Turkey*

Article Info

Research article
Received: 01/11/2024
Revision: 18/12/2024
Accepted: 18/12/2024

Keywords

Double-FG Material
GPL-Reinforced Nanoplate
Ti-6Al-4V
Silicon Nitride

Makale Bilgisi

Araştırma makalesi
Başvuru: 01/11/2024
Düzeltme: 18/12/2024
Kabul: 18/12/2024

Anahtar Kelimeler

Çift-FD Malzeme
GPL-Takviyeli Nanoplaka
Ti-6Al-4V
Silikon Nitrür

Graphical/Tabular Abstract (Grafik Özet)

In this article, the variation in mechanical and thermal material properties of double functionally graded composite nanoplates reinforced with graphene platelets subjected to thermal loading is investigated. / Bu makalede, termal yüklemeye maruz kalan grafen plakalar ile güçlendirilmiş çift fonksiyonel derecelendirilmiş kompozit nanoplakaların mekanik ve termal malzeme özelliklerindeki değişim incelenmiştir.

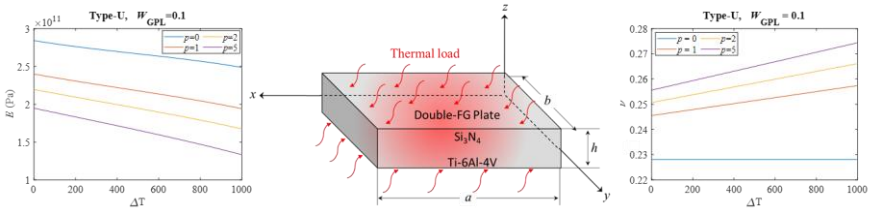

***Figure A**: Investigation of mechanical and thermal material properties of GPL-reinforced double-FG composite nanoplates / **Şekil A:** GPL ile güçlendirilmiş çift-FD kompozit nanoplakaların mekanik ve termal malzeme özelliklerinin incelenmesi*

Highlights (Önemli noktalar)

- *Halpin-Tsai micromechanical procedures, power-law distribution, and law of mixtures are employed to determine the effective properties of the proposed plate structure. / Önerilen plakanın efektif özelliklerini belirlemek için Halpin-Tsai mikromekanik prosedürü, power-law dağılımı ve karışımlar kanunu uygulanmıştır.*
- *Higher modulus of elasticity values are obtained in the Type-X dispersion model. Also, while modulus of elasticity decreases with temperature rise and power law parameter, it increases with GPL weight ratio. / Tip-X dağılım modelinde daha yüksek elastisite modülü değerleri elde edilmiştir. Ayrıca, elastisite modülü sıcaklık artışı ve kuvvet yasası parametresi ile azalırken, GPL ağırlık oranı ile artmaktadır.*
- *Higher values of the thermal expansion coefficient are observed in the Type-U dispersion model. / Tip-U dağılım modelinde daha yüksek termal genleşme katsayısı gözlenmiştir.*
- *Increasing power law index and GPL weight ratio increases the effective thermal conductivity coefficient of the composite plate. / Artan kuvvet yasası indeksi ve GPL ağırlık oranı, kompozit plakanın etkin termal iletkenlik katsayısını artırmaktadır.*

***Aim (Amaç):** This article aims to analyze the change in mechanical and thermal material properties of double functionally graded composite nanoplates reinforced with graphene platelets subjected to thermal loading. / Bu makale, termal yüklemeye maruz kalan grafen plakalarla güçlendirilmiş çift fonksiyonel dereceli kompozit nanoplakaların mekanik ve termal malzeme özelliklerindeki değişimi analiz etmeyi amaçlamaktadır.*

***Originality (Özgünlük):** The investigation of the thermal and mechanical properties of the presented double-FG GPLs-reinforced plate by considering the temperature dependent material properties is a subject that wasn't studied previously. / Sunulan çift-FD GPL takviyeli plakanın termal ve mekanik özelliklerinin sıcaklığa bağlı malzeme özellikleri dikkate alınarak incelenmesi daha önce çalışılmamış bir konudur.*

***Results (Bulgular):** According to analysis, it is determined that the thermal and mechanical characteristics of the plate change significantly with temperature rise and exhibit quite different performance at room temperature and high temperature environments. / Analiz sonuçlarına göre, plakanın termal ve mekanik özelliklerinin sıcaklık artışıyla önemli ölçüde değiştiği ve oda sıcaklığı ile yüksek sıcaklık ortamlarında oldukça farklı performans sergilediği tespit edilmiştir.*

***Conclusion (Sonuç):** With this work, it is expected to provide contribution to aerospace, marine and medical applications, micro and nano electromechanical devices that will operate in environments requiring high temperature and corrosion resistance. / Bu çalışma ile yüksek sıcaklık ve korozyon direnci gerektiren ortamlarda çalışacak havacılık, denizcilik ve medikal uygulamalara, mikro ve nano elektromekanik cihazlara, önemli katkı sağlanması beklenmektedir.*

*Corresponding author, e-mail: kerimgokhanaktas@karabuk.edu.tr
DOI: 10.29109/gujsc.1577831

GU J Sci, Part C, 13(1): 341-354 (2025)

Gazi Üniversitesi
Fen Bilimleri Dergisi
PART C: TASARIM VE TEKNOLOJİ

Gazi University
Journal of Science
PART C: DESIGN AND TECHNOLOGY

http://dergipark.gov.tr/gujsc

Analysis of Mechanical and Thermal Material Characteristics of GPL-Reinforced Double-FG Composite Nanoplates under Temperature Load

Kerim Gökhan AKTAŞ[1*]

[1]*Karabuk University, Faculty of Engineering, Department of Mechanical Engineering, Karabuk, Turkey*

Article Info

Research article
Received: 01/11/2024
Revision: 18/12/2024
Accepted: 18/12/2024

Keywords

Double-FG Material
GPL-ReinforcedNanoplate
Ti-6Al-4V
Silicon Nitride

Abstract

This article analyzes the variation in the mechanical and thermal material characteristics of graphene platelets (GPLs)-reinforced double-functionally graded (FG) composite nanoplates subjected to thermal load. Titanium alloy Ti-6Al-4V and silicon nitride (Si_3N_4) metal-ceramic matrix is preferred for the nanoplate matrix due to their potential for use in thermal environments. The double-FG properties of the structure are provided by the functional dispersion of the ceramic-metal matrix as well as the effective arrangement of the GPLs in two distinct patterns throughout the plate's thickness (Type-X and Type-U). The thermal and mechanical characteristics of the matrix materials and GPLs are temperature-dependent. The effective material properties of the double-FG nanoplate matrix are obtained using Voigt's rule of mixture. The analysis is conducted to evaluate the influence of variables like temperature rise, GPLs weight ratio and GPLs distribution patterns on the thermal and mechanical properties of the nanoplate such as effective modulus of elasticity, Poisson's ratio, coefficient of thermal expansion and coefficient of thermal conductivity. According to the results of the analysis, it is determined that the thermal and mechanical characteristics of the proposed plate change significantly with temperature rise and exhibit quite different performance at room temperature and high temperature environments. With the presented work, it is expected to provide significant contribution to aerospace, marine and medical applications, micro and nano electromechanical devices, microprocessors and transistors that will operate in environments requiring high temperature and corrosion resistance.

Sıcaklık Yükü Etkisi Altındaki GPL Takviyeli Çift-FD Kompozit Nanoplakaların Mekanik ve Termal Malzeme Özelliklerinin Analizi

Makale Bilgisi

Araştırma makalesi
Başvuru: 01/11/2024
Düzeltme: 18/12/2024
Kabul: 18/12/2024

Anahtar Kelimeler

Çift-FD Malzeme
GPL-Takviyeli Nanoplaka
Ti-6Al-4V
Silikon Nitrür

Öz

Bu makale, termal yüke maruz kalan grafen nano plaka (GPL) takviyeli çift fonksiyonel derecelendirilmiş (FD) nano plakaların mekanik ve termal malzeme özelliklerindeki değişimini analiz etmektedir. Termal ortamlarda kullanım potansiyelleri nedeniyle titanyum alaşımı Ti-6Al-4V ve silikon nitrür (Si_3N_4) metal-seramik matrisi, nano plaka matrisi için tercih edilmiştir. Plakanın çift-FG özellikleri, seramik-metal matrisin fonksiyonel dağılımının yanı sıra GPL'lerin plaka kalınlığı boyunca iki farklı düzende (Tip-X ve Tip-U) fonksiyonel bir şekilde düzenlenmesiyle sağlanmaktadır. Matris malzemelerinin ve GPL'lerin termal ve mekanik özellikleri sıcaklığa bağlıdır. Çift-FD nanoplaka matrisinin etkin malzeme özellikleri Voigt'in karışım kuralı kullanılarak elde edilmiştir. Analiz çalışmaları, sıcaklık artışı, GPL ağırlık oranı ve GPL dağılım paternleri gibi değişkenlerin nanoplakanın efektif elastisite modülü, Poisson oranı, termal genleşme katsayısı ve termal iletkenlik katsayısı gibi termal ve mekanik özellikleri üzerindeki etkisini değerlendirmek için gerçekleştirilmiştir. Analiz sonuçlarına göre, önerilen plakanın termal ve mekanik özelliklerinin sıcaklık artışı ile önemli ölçüde değiştiği ve oda sıcaklığı ile yüksek sıcaklık ortamlarında oldukça farklı performans sergilediği tespit edilmiştir. Sunulan çalışma ile havacılık, denizcilik ve medikal uygulamalara, yüksek sıcaklık ve korozyon direnci gerektiren ortamlarda çalışacak mikro ve nano elektromekanik cihazlara, mikroişlemcilere ve transistörlere önemli katkı sağlanması beklenmektedir.

1. INTRODUCTION (GİRİŞ)

The special thermal and mechanical characteristics of functionally graded materials (FGMs) make them highly attractive for use in engineering applications where improved performance is required in a wide range of environments. Mechanical and thermal characteristics of FGMs change regularly along the

*Corresponding author, e-mail: kerimgokhanaktas@karabuk.edu.tr
DOI: 10.29109/gujsc.1577831

material's thickness direction due to the material's composition, which vary gradually. Material performance in fields including structural engineering, civil engineering, aerospace, and automotive can be modified by adjusting this gradient [1,2]. The mechanical properties of FGMs can be described through various methodologies, including power-law distributions, which represent the variation of parameters such as Young's modulus, Poisson's ratio and density between different surfaces. For example, Arefi's research [3] on functionally graded sandwich plates incorporating piezoelectric layers demonstrates the application of a power law function to depict the arrangement of mechanical characteristics, with the bottom surface composed of steel and the top layer of ceramic. This methodology is essential for comprehending the behavior of FGMs under mechanical stresses, as it facilitates the estimation of stress and deformation parameters that considerably vary from those of homogeneous elements [4]. Thermal characteristics of FGMs are also essential, especially in applications where temperature gradients exist. Findings from FGM thermal stress analyses show that residual stresses and thermal adaptability are strongly affected by the in-plane material composition gradient [5].

GPLs have become a crucial reinforcement material in different composite materials, especially in the manufacturing of graphene-reinforced plate structures. The integration of GPLs into composite structures has been thoroughly examined owing to their remarkable mechanical features, which encompass enhanced tensile strength, rigidity, and thermal conductivity. Due to these qualities, GPLs are an appealing option for improving the functionality of composites made of polymers and metals. The mechanical reinforcement provided by graphene is used in various structures. For example, the total mechanical characteristics of the composite are greatly improved as a result of the effective load transfer that occurs between the GPLs and the matrix material. This effect has been observed in research that evaluated the mechanical behavior of FG porous components that were reinforced with GPLs. The results of these studies demonstrated better stiffness and strength properties in comparison to their counterparts that were not reinforced [6–9]. The uniform distribution of GPLs within the matrix is essential for enhancing mechanical achievement, as it reduces deficiencies and improves interfacial bonding, which is critical for stress transmission [10,11]. The incorporation of GPLs into metal matrix composites has led to significant enhancements in mechanical characteristics. Researchers has shown that composites containing graphene and metals, such as aluminum and copper, have higher tensile strength and hardness than those without graphene [12,13].

Dual functionally graded materials signify a notable progression in material science, integrating the distinct features of multiple materials in a gradient configuration to attain improved performance attributes [14]. The principal benefit of FGMs is their capacity to customize material qualities, including thermal resistance, mechanical strength, and wear resistance, by altering the composition and microstructure across the material [15]. Additionally, the incorporation of advanced materials such as graphene and carbon nanotubes into FGMs has been investigated to improve their mechanical and thermal characteristics. The integration of carbon nanotubes into ceramic materials enhances their mechanical properties and thermal stability, as reported by Estili and Sakka [16]. The vibration of a smart sandwich plate with auxetic core and dual-FG nanocomposite layers integrated with piezoceramic actuators has been studied by Nouraei et al [17]. Shen [18] proposed the idea of FG-CNT reinforced nanocomposites, wherein the CNTs are distributed throughout the structure's thickness using various FG patterns. Kamarian et al. [19] examined the impact of the temperature environment on the buckling behavior of a sandwich plate featuring FG-CNT reinforced nanocomposite face sheets.

Si_3N_4 is a ceramic substance that has attracted considerable interest owing to its remarkable thermal and mechanical characteristics, rendering it appropriate for many applications in engineering and materials research. Si_3N_4 possesses exceptional strength, toughness, and hardness, essential for use in challenging conditions. The thermal characteristics of Si_3N_4 are also remarkable. It has a high thermal conductivity that enables efficient heat dissipation in high-temperature applications. This feature is especially advantageous in electrical and aeronautical applications where temperature management is essential [20]. The improved strength-to-weight ratio facilitates the creation of lightweight constructions without reducing performance. Moreover, thermal shock resistance of Si_3N_4 enhances its utility in demanding environments, particularly within the aerospace and automotive fields [21]. Ti-6Al-4V is highly regarded for its outstanding thermal and mechanical characteristics, rendering it a preferred material in several technical applications, especially in aerospace and biomedical sectors. The alloy's composition provides high strength-to-weight ratio and corrosion resistance for high-performance

applications [22]. Ti-6Al-4V demonstrates comparatively low heat conductivity relative to other metals, which might be beneficial in applications requiring thermal insulation. The thermal expansion coefficient of Ti-6Al-4V is an essential parameter, especially in applications with temperature variations, since it can cause dimensional modifications that may impact construction and efficiency [23]. The Ti-6Al-4V and Si_3N_4 FGMs are of particular interest as they combine the high strength and ductility of the titanium alloy with the excellent thermal and wear resistance of the silicon nitride ceramic. These materials exhibit superior performance in terms of thermal protection, mechanical strength, and resistance to stress concentration, making them attractive for a wide range of applications, including aerospace, energy, and biomedical industries [24]. Materials with high temperature strength and corrosion resistance are required for applications involving severe temperature technology, such as aerospace, because of their extraordinary high temperature qualities, great mechanical capabilities, and high toughness and strength [25]. Conventional Si_3N_4 ceramics have low fracture toughness, as do most ceramics [26]. As a result, it is unavoidable to employ FGM structures to combine the superior mechanical and thermal capabilities of ceramic and metal materials.

As mentioned above, the mechanical and thermal properties of FG plates can vary considerably via temperature. Therefore, the issue important to include temperature dependent substance properties in the mechanical and thermal inspection of components operating in low and high temperature regions. By conducting a comprehensive review of the existing literature, it is concluded that the investigation of the thermal and mechanical properties of the presented double-FG GPLs-reinforced plate by considering the temperature dependent material properties is a subject that wasn't studied previously. Si_3N_4 and Ti-6Al-4V titanium alloy have been selected as the matrix materials of the proposed plate, which can be used in many engineering fields due to their superior mechanical and thermal properties. It is expected that the proposed study will contribute to high temperature and corrosion applications in nanoelectromechanical systems, aerospace, marine and medical applications.

2.THEORY AND FORMULATION (TEORİ VE FORMÜLASYON)

2.1. A Summary of the Proposed Double-FG Nanoplate (Önerilen Çift-FD Nanoplakanın Özeti)

The current investigation presents a FGM nanostructure characterized by dimensions length a, width b, and thickness h, as illustrated in Figure 1. The middle layer of the FGM plate contains the in-plane coordinates x and y, while the direction z extends across the thickness of plate. The nanoplate is under thermal load along the z-axis. Two distinct patterns of GPL distribution are proposed to reinforce the FG metal-ceramic matrix in the plate layer. As illustrated in Figure 2, these patterns comprise functionally graded distribution (Type-X) along the thickness axis and a uniform distribution (Type-U).

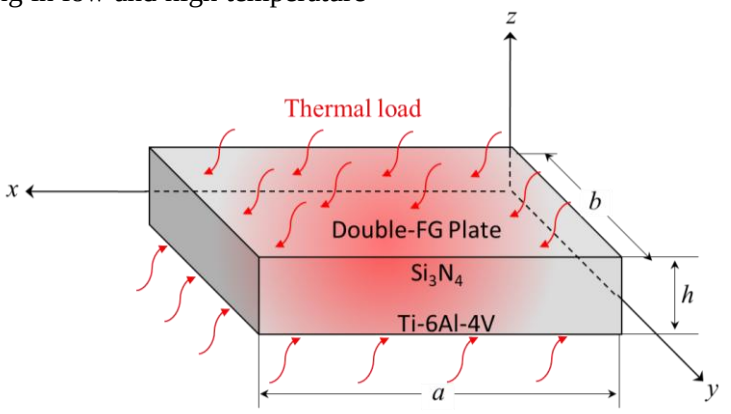

Figure 1. GPL-reinforced double-FG nanoplate structure (GPL ile güçlendirilmiş çift-FD nanoplaka yapı)

2.2. Double-FG Properties (Çift-FD Özellikler)

Introducing GPLs with functionally graded dispersion arrangement within FG Si_3N_4/Ti-6Al-4V core results in the double-FG characteristics of the suggested nanostructure. The double-FG plate structure consists of a ceramic (Si_3N_4) and a metal (Ti-6Al-4V) matrix. The effective mechanical and thermal properties of the nanoplate are graded using power law dispersion. The top surface of the FGM plate is defined as Si_3N_4, and the bottom surface as Ti-6Al-4V. The efficient features of the nanoplate matrix determined using the law of mixtures as follows [27]:

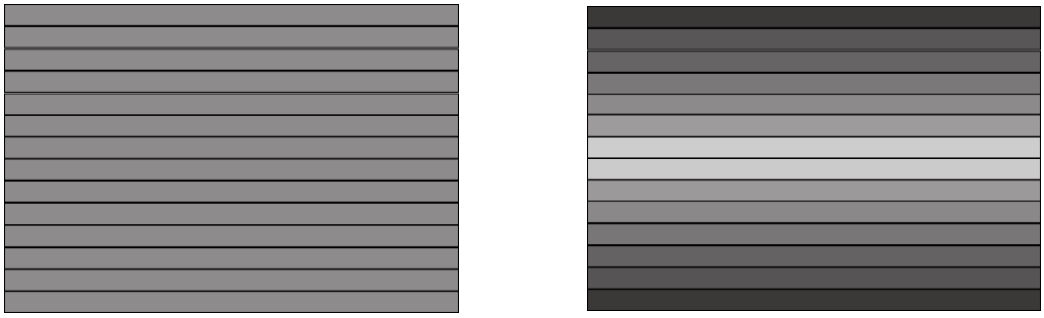

Type-U Type-X

Figure 2. GPL dispersion patterns (GPL dağılım paternleri)

$$E_{matrix} = E_{met} + (E_{cer} - E_{met})V_{cer} \quad (1)$$

$$v_{matrix} = v_{met} + (v_{cer} - v_{met})V_{cer} \quad (2)$$

$$\rho_{matrix} = \rho_{met} + (\rho_{cer} - \rho_{met})V_{cer} \quad (3)$$

$$\alpha_{matrix} = \alpha_{met} + (\alpha_{cer} - \alpha_{met})V_{cer} \quad (4)$$

$$\kappa_{matrix} = \kappa_{met} + (\kappa_{cer} - \kappa_{met})V_{cer} \quad (5)$$

where cer denotes a ceramic matrix and met denotes a metal matrix. Furthermore, the ρ_{matrix}, v_{matrix}, α_{matrix}, κ_{matrix}, and E_{matrix} indicate the effective properties of nanoplate matrix. The subsequent method can be utilized in order to ascertain the volume ratio of the ceramic, indicated as V_{cer}, using the power-law distribution [17,27]:

$$V_{cer} = \left(\frac{1}{2} + \frac{z}{h}\right)^{p} \quad h_1 \leq z \leq h_2 \quad (6)$$

in which $h_1 = -h/2$ and $h_2 = +h/2$. The variable z represents the location toward the neutral axis, whereas the variable n symbolizes the power-law variable.

2.3. Distribution Patterns for GPLs (GPL'ler için Dağılım Paternleri)

Employing the following steps of the Halpin-Tsai micromechanical processes, the modulus of elasticity of the GPL-reinforced nanoplate can be determined as [28]:

$$E = \frac{3}{8}\left(\frac{\xi_L \eta_L V_{GPL}}{1 - \eta_L V_{GPL}}\right) E_{matrix} + \frac{5}{8}\left(\frac{1 + \xi_w \eta_w V_{GPL}}{1 - \eta_w V_{GPL}}\right) E_{matrix} \quad (7)$$

$$\xi_L = \frac{2l_{GPL}}{t_{GPL}} \quad (8)$$

$$\xi_w = \frac{2w_{GPL}}{t_{GPL}} \quad (9)$$

$$\eta_L = \frac{(E_{GPL}/E_{matrix}) - 1}{(E_{GPL}/E_{matrix}) + \xi_L} \quad (10)$$

$$\eta_w = \frac{(E_{GPL}/E_{matrix}) - 1}{(E_{GPL}/E_{matrix}) + \xi_w} \quad (11)$$

The parameters w_{GPL}, l_{GPL}, and t_{GPL} symbolize the GPLs' width, length, and thickness, respectively. The GPLs' modulus of elasticity is also denoted by E_{GPL}. The following equation could be used to compute the thermal and mechanical parameters of the nanoplate that has been reinforced with GPL [28]:

$$v = v_{GPL}V_{GPL} + v_{matrix}V_{matrix} \quad (12)$$

$$\rho = \rho_{GPL}V_{GPL} + \rho_{matrix}V_{matrix} \quad (13)$$

$$\alpha = \alpha_{GPL}V_{GPL} + \alpha_{matrix}V_{matrix} \quad (14)$$

$$\kappa = \kappa_{GPL}V_{GPL} + \kappa_{matrix}V_{matrix} \quad (15)$$

$$V_{matrix} = 1 - V_{GPL} \quad (16)$$

V_{GPL} and V_{matrix} stand for the volume ratio of the GPLs and Si_3N_4/Ti-6Al-4V core, respectively. While GPLs are evenly distributed in the Type-U arrangement, the Type-X arrangement exhibits a declining GPL weight fraction between the lower and upper surfaces to the center layers. The Type-X design shows a declining GPL ratio from the lower and upper surfaces to the center, whereas GPLs are

evenly distributed in the Type-U distribution pattern. For Type-U model [29]:

$$V_{GPL}^{*} = \frac{\rho_{matrix} W_{GPL}}{\rho_{matrix} W_{GPL} + \rho_{GPL}(1 - W_{GPL})} \quad (17)$$

where the weight ratio of the GPLs is expressed by W_{GPL}, whereas the density of the GPLs is expressed by ρ_{GPL}. For the Type-X model [30]:

$$V_{GPL}(z) = V_{GPL}^{*}\left[1 - \cos\left(\frac{z\pi}{\mathrm{h}}\right)\right] \quad h_1 \le z \le h_2 \quad (18)$$

The physical characteristics of the double-FG nanoplate are temperature dependent. The mechanical and thermal characteristics can be expressed through a nonlinear temperature equation that incorporates E, υ, κ, and α as follows [31–33]:

$$P = P_0(P_{-1}T^{-1} + 1 + P_1 T + P_2 T^2 + P_3 T^3) \quad (19)$$

where $T = T_0 + \Delta T$ and $T_0 = 300$ K. P_0, P_{-1}, P_1, P_2, and P_3 denote the temperature-dependent material constants. The material constants of Si_3N_4, Ti-6Al-4V, and GPLs in which vary with temperature are listed in Table 1. The temperature is regarded as exhibiting a nonlinear change. Under certain temperature constraints, Eq. (19) can be computed to find the top and bottom layer temperatures (T_t and T_b) of the plate [34].

$$-\frac{d}{dz}\left[\kappa(z,T)\frac{dT}{dz}\right] = 0, \quad T\left(\frac{h}{2}\right) = T_t, \quad T\left(-\frac{h}{2}\right) = T_b \quad (20)$$

3.NUMERICAL RESULTS AND DISCUSSION
(SAYISAL SONUÇLAR VE TARTIŞMA)

In this section, the temperature-dependent effective material coefficients of the double-FG nanoplate are analyzed under thermal loads. The fundamental parameters of the nanostructure employed in the calculations are specified as $a = b = 500$ nm, $h = a/10$. Furthermore, the physical parameters of the GPLs are assumed to be l_{GPL} =2.5 nm, w_{GPL} =1.5 nm, and t_{GPL} =0.2 nm. According to the literature, rising nanofiller concentration causes agglomeration, which reduces the mechanical characteristics of nanocomposites [35,36]. For this reason, the plate dimensions of the presented sandwich structure are chosen in such a way that the GPL effect can be clearly observed, and the agglomeration problem can be avoided.

Table 1. Mechanical and thermal constants of Si_3N_4/Ti-6Al-4V and GPL [33,37] (Si_3N_4/Ti-6Al-4V ve GPL'nin mekanik ve termal sabitleri)

Material	Properties	P_{-1}	P_0	P_1	P_2	P_3
Si_3N_4	E (Pa)	0	348.43x10^9	-3.070x10^{-4}	2.160x10^{-7}	-8.946x10^{-11}
	υ	0	0.24	0	0	0
	α (K^{-1})	0	5.8723x10^{-6}	9.095x10^{-4}	0	0
	κ (W/mk)	0	13.723	-1.032x10^{-3}	5.466x10^{-7}	-7.876x10^{-11}
	ρ (kg/m^3)	0	2370	0	0	0
Ti-6Al-4V	E (Pa)	0	122.56x10^9	-4.586x10^{-4}	0	0
	υ	0	0.2884	1.121x10^{-4}	0	0
	α (K^{-1})	0	7.5788x10^{-6}	6.638x10^{-4}	-3.147x10^{-6}	0
	κ (W/mk)	0	1	1.704x10^{-2}	0	0
	ρ (kg/m^3)	0	4512	0	0	0
GPLs	E (Pa)	0	1087.8x10^9	-0.261x10^9	0	0
	υ	0	0.186	0	0	0
	α (K^{-1})	0	13.92x10^{-6}	-0.029x10^{-6}	0	0
	κ (W/mk)	0	2200	6.739x10^{-2}	-2.585x10^{-4}	0
	ρ (kg/m^3)	0	1060	0	0	0

3.1. Validation of the Proposed Methodology
(Önerilen Metodolojinin Doğrulanması)

To validate the proposed technique, a comparison is conducted with the current literature. In the first verification analysis, the dimensionless natural frequencies of multilayer functionally graded GPL/polymer plates with various GPL distribution arrangements are examined and compared with the results of Song et al [38]. Epoxy is preferred as the polymer matrix in the study. The dimensions of the plate are taken as a=0.45 m, b=0.45 m and h=0.045 m, and the dimensions of the GPLs are taken as l_{GPL}=2.5 μm, w_{GPL}=1.5 μm and h_{GPL}=1.5 nm. In addition, the mechanical properties of GPL and matrix are considered as E_{GPL}=1.01 TPa, ρ_{GPL}=1.06 g/cm^3, υ_{GPL}=0.186, E_M=3 GPa, ρ_M=1.2 g/cm^3,and υ_m=0.34. The obtained dimensionless natural frequencies are compared with reference work in Table 2. As shown in the table, there is a high similarity between the natural frequency values. In the second validation study, the free vibration response of graphene platelet reinforced composite plates is investigated for different GPL distributions under the influence of temperature and compared with the results of Quaderi et al. [39]. In the study, GPLs are assumed to be dispersed in the epoxy matrix. Two different GPL patterns are discussed in comparison. In Pattern 1, the GPLs are homogeneously distributed, while in Pattern 2, the GPL weight ratio is higher in the center of the plate and decreases towards the top and bottom surface. The plate dimensions and material properties are the same as in the first validation study. As shown in Table 3, the natural frequency results obtained from the presented study and the reference study are in good agreement with each other.

Table 2. Comparison of dimensionless natural frequency $\bar{w} = w\sqrt{\rho_M/E_M}$ values for different GPL distributions. (Farklı GPL dağılımları için boyutsuz doğal frekans değerlerinin karşılaştırılması)

	Pattern 1		**Pattern 2**		**Pattern 3**	
Mode (m,n)	Ref. [38]	Present	Ref. [38]	Present	Ref. [38]	Present
(1,1)	0.1216	0.1288	0.1020	0.1104	0.1378	0.1487
(2,2)	0.4436	0.4578	0.3796	0.3935	0.4939	0.5133
(3,3)	0.8869	0.9123	0.7755	0.7901	0.9690	0.9814

Table 3. Validation of natural frequency values for temperature increase (Sıcaklık artışı için doğal frekans değerlerinin doğrulanması)

			Pattern 1		**Pattern 2**	
a/h	a/b	ΔT	Ref. [39]	Present	Ref. [39]	Present
10	1	0	1300	1299	1145	1143
		30	1194	1191	1023	1022
		60	1078	1080	885	882
		90	948	946	721	718
5	1	0	2368	2367	3104	3104
		30	2313	2311	3064	3062
		60	2257	2255	3024	3025
		90	2200	2197	2984	2981

Table 4. Comparison of the effective modulus of elasticity and coefficient of thermal conductivity of Si_3N_4 plate (Si_3N_4 plakanın efektif elastisite modülü ve termal iletkenlik katsayısının karşılaştırılması)

	E **(Pa)**		κ **(W/mK)**	
ΔT	Ref. [40]	Present	Ref. [40]	Present
300	$3.05\text{x}10^{11}$	$3.03\text{x}10^{11}$	$0.82\text{x}10^{-5}$	$0.83\text{x}10^{-5}$
400	$2.97\text{x}10^{11}$	$2.92\text{x}10^{11}$	$0.89\text{x}10^{-5}$	$0.93\text{x}10^{-5}$
500	$2.92\text{x}10^{11}$	$2.90\text{x}10^{11}$	$0.98\text{x}10^{-5}$	$1.01\text{x}10^{-5}$
600	$2.88\text{x}10^{11}$	$2.83\text{x}10^{11}$	$1.09\text{x}10^{-5}$	$1.18\text{x}10^{-5}$
700	$2.83\text{x}10^{11}$	$2.80\text{x}10^{11}$	$1.19\text{x}10^{-5}$	$1.24\text{x}10^{-5}$
800	$2.79\text{x}10^{11}$	$2.75\text{x}10^{11}$	$1.31\text{x}10^{-5}$	$1.35\text{x}10^{-5}$

In order to ensure the accuracy of the temperature dependent material properties and temperature equations, modulus of elasticity values and thermal expansion coefficients of Si_3N_4 plate are determined in the range of ΔT =300-800 K and the obtained results are compared with the analytical results of Koç et al. [40]. According to the data obtained from Table 4, it is seen that the results of the two studies are quite convergent.

3.2. Effective Material Properties of the Double-FG Plate (Çift-FD Plakanın Efektif Malzeme Özellikleri)

This chapter determines the temperature-dependent effective material properties of the double-FG nanoplate, utilizing different power law indices p and GPL weight fractions, while comparing two distinct GPL distribution methods (Type-U and Type-X). Analytical investigations are conducted for four specific power law values (p=0, 1, 2, and 5) within the temperature range of 0 K to 1000 K. In addition, the GPL weight ratio gradually increased from 0 to 0.2. The material properties of GPL-reinforced double-FG nanoplate gradually approach from Si_3N_4 to Ti-6Al-4V with rising p.

The variation of the effective modulus of elasticity with respect to temperature rise ΔT, GPL weight fraction W_{GPL} and GPL distribution patterns (Type-U and Type-X) are depicted in Figure 3. The evaluation of Figure 3a and Figure 3c indicate that the modulus of elasticity of the FG plate significantly diminishes with rising temperature in both Type-U and Type-X distribution patterns. Furthermore, as the power law parameter increases, the modulus of elasticity decreases. The drop is attributed to the dominance of the Ti-6Al-4V characteristics of the plate as the power law index increases. The modulus of elasticity value of Si_3N_4 is significantly greater than that of Ti-6Al-4V, as indicated in Table 1. In addition, a comparison of Type-X and Type-U dispersion models with same ΔT and p values reveals that the Type-X dispersion model yields higher modulus of elasticity values. When Figure 3b and Figure 3d are evaluated, modulus of elasticity values of the nanoplate increase significantly with increasing W_{GPL}. From the comparison of Type-X and Type-U concepts for W_{GPL} = 0.2, it is apparent that higher E values are obtained in the Type-X.

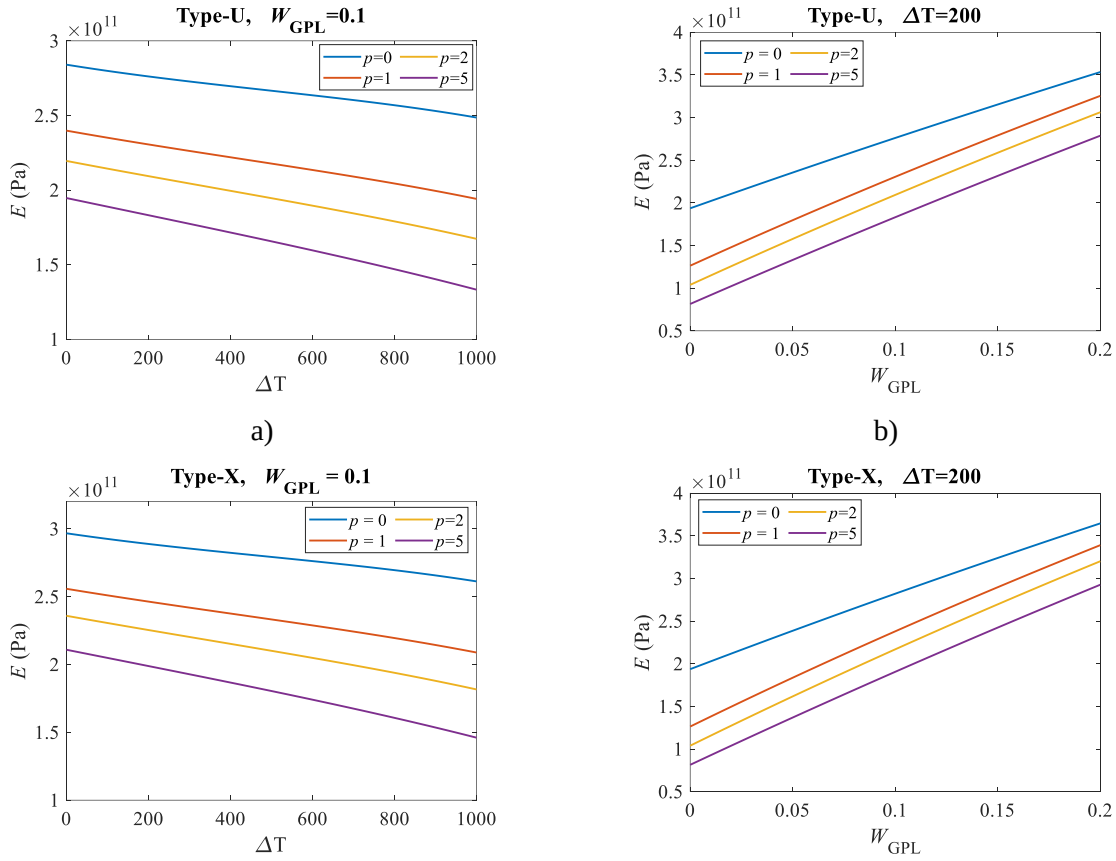

Figure 3. Evaluation of the effective modulus of elasticity depending on ΔT and W_{GPL} for Type-U and Type-X dispersion models (Tip-U ve Tip-X dağılım modelleri için ΔT ve W_{GPL}'ye bağlı olarak etkin elastisite modülünün değerlendirilmesi)

Figure 4 illustrates the variation of effective Poisson's ratio of the FG nanoplate according to temperature increase ΔT, GPL weight ratio W_{GPL}. As shown in Figure 4a and Figure 4c, the effective Poisson's ratio of the plate increases with increasing temperature for p=1, 2 and 5. For p=0, the Poisson's ratio remains constant. This is because at p=0 the plate is completely composed of Si_3N_4. Moreover, when the Type-X and Type-U GPL dispersion models are examined for the same ΔT and p, it is observed that higher Poisson's ratio values are achieved in the Type-U dispersion model. As seen in Figure 4b and Figure 4d, increasing GPL weight ratio has a decreasing effect on Poisson's ratio value. The comparison of Type-X and Type-U distribution patterns for W_{GPL} = 0.2 reveals that the Type-U dispersion model provides greater Poisson's ratio values.

Figure 5 evaluates the fluctuation of the efficient thermal expansion parameter of double-FG nanoplate with increasing temperature, power law index and GPL weight ratio. As simulated in Figure 5a and Figure 5c, increasing power law index and temperature have an increasing effect on the thermal expansion constant. In Type-U dispersion scheme, a 221.55% increase in the thermal expansion coefficient is observed for p=0, while a 49.42% increase is observed for p=5. This difference is due to the variation in the temperature dependent thermal expansion coefficients of Si_3N_4 and Ti-6Al-4V matrices with the applied thermal load. Furthermore, as it is clearly seen from the figures, higher thermal expansion coefficients are achieved in Type-U compared to the Type-X, especially at higher power law index values. Figure 5b and Figure 5d demonstrate that the effective thermal expansion of the plate rises with an increasing GPL weight ratio at p=0 and p=1 power law parameters, however it remains almost constant at p=2 and decreases at p=5. The fluctuation is attributable to the GPL thermal expansion coefficient being lower than that of Ti-6Al-4V and higher than that of Si_3N_4. Furthermore, Figure 5d shows that the GPL distribution pattern has no significant effect on the effective coefficient of thermal expansion except for the case where the plate has an all-ceramic matrix (p=0).

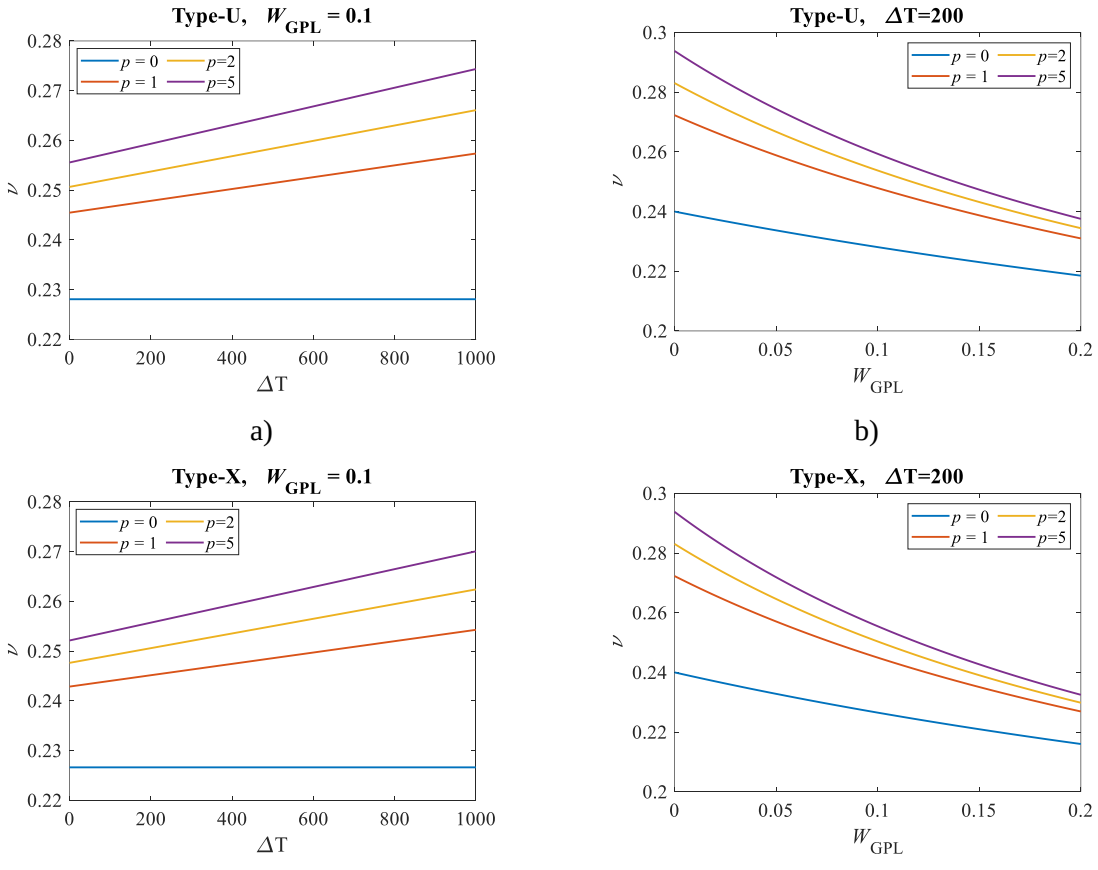

Figure 4. Evaluation of the effective Poisson's ratio depending on ΔT and W_{GPL} for Type-U and Type-X dispersion models (Tip-U ve Tip-X dağılım modelleri için ΔT ve W_{GPL}'ye bağlı olarak etkin Poisson oranının değerlendirilmesi)

Figure 6 presents the variation of the effective thermal conductivity coefficient of the proposed double-FG nanoplate with respect to parameters ΔT, p and W_{GPL}. As presented in Figure 6a and Figure 6c, the effective thermal conductivity coefficient of the plate decreases with increasing temperature. Considering the plate components Si_3N_4, Ti-6Al-4V and GPL separately and analyzing the thermal conductivity coefficients from Table 1 and Eq. (19), it is seen that the thermal conductivity coefficients of Si_3N_4 and GPL tend to decrease while the thermal conductivity coefficient of Ti-6Al-4V tends to increase. However, due to the superior thermal conductivity properties of GPL compared to other components, it is clearly seen that the FG plate shows a similar trend to the GPL behavior for thermal conductivity. Moreover, as depicted, the thermal conductivity coefficient of the double-FG nanostructure rises with increasing power law index. As given in Table 1, the initial Si_3N_4 thermal conductivity coefficient is higher than that of Ti-6Al-4V. However, despite this, lower values are obtained at p=0 than at p=5 because the density of Ti-6Al-4V is almost twice that of the ceramic matrix, which results in a higher V_{GPL} value. As illustrated in Figure 6b and Figure 6d, the effective thermal conductivity coefficient of the FG plate increases significantly with increasing W_{GPL}.When W_{GPL} =0 and W_{GPL}=0.2 values are compared at power law parameter p=5, it is found that the thermal conductivity value of the plate increases from approximately 6.78 W/mK to 1079.8 W/mK. It is also found from the figures that with increasing temperature, the thermal conductivity coefficient decreases more in the Type-X than in the Type-U due to the percentage of GPL on the upper and lower surfaces of the plate, and similarly, with increasing W_{GPL}, the thermal conductivity coefficient increases more in the Type-X model.

To make the findings more versatile for different applications, the effect of high temperature and GPL ratio on the effective modulus of elasticity is presented in Figure 7. As shown in the figure, while there is a linear decrease until approximately ΔT =1000 K, it shows nonlinear behavior after this value. Also, for lower values of W_{GPL}, the difference between p=0 and p=5 curves are quite large, while for high values of W_{GPL} this difference decreases significantly.

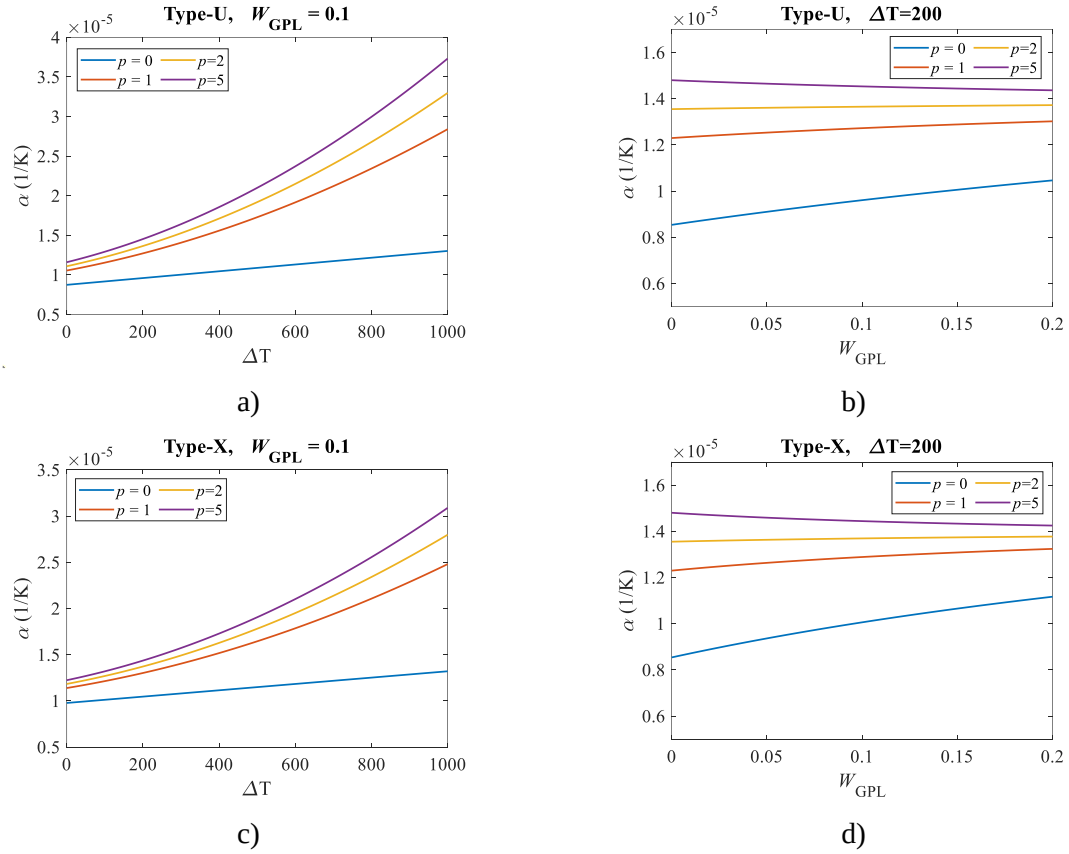

Figure 5. Evaluation of the thermal expansion coefficient depending on ΔT and W_{GPL} for Type-U and Type-X dispersion models (Tip-U ve Tip-X dağılım modelleri için termal genleşme katsayısının değerlendirilmesi)

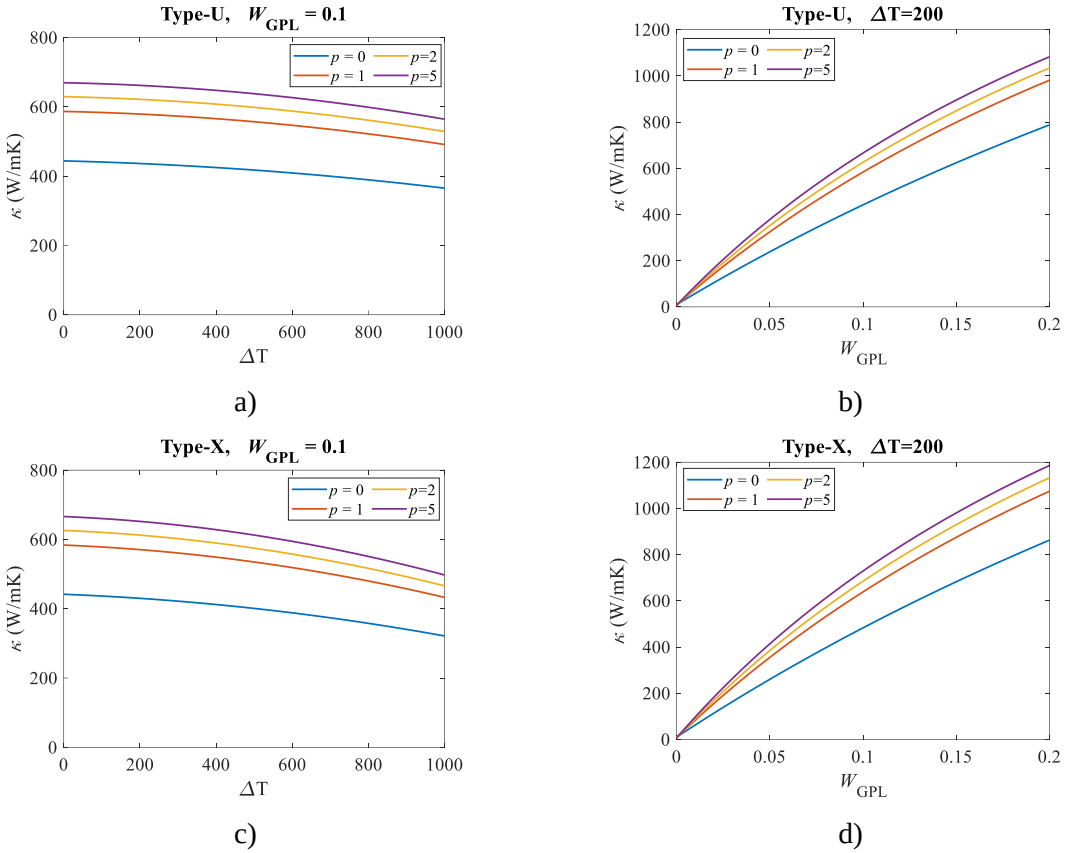

Figure 6. Evaluation of the thermal conductivity coefficient depending on ΔT and W_{GPL} for Type-U and Type-X dispersion models (Tip-U ve Tip-X dağılım modelleri için termal iletkenlik katsayısının değerlendirilmesi)

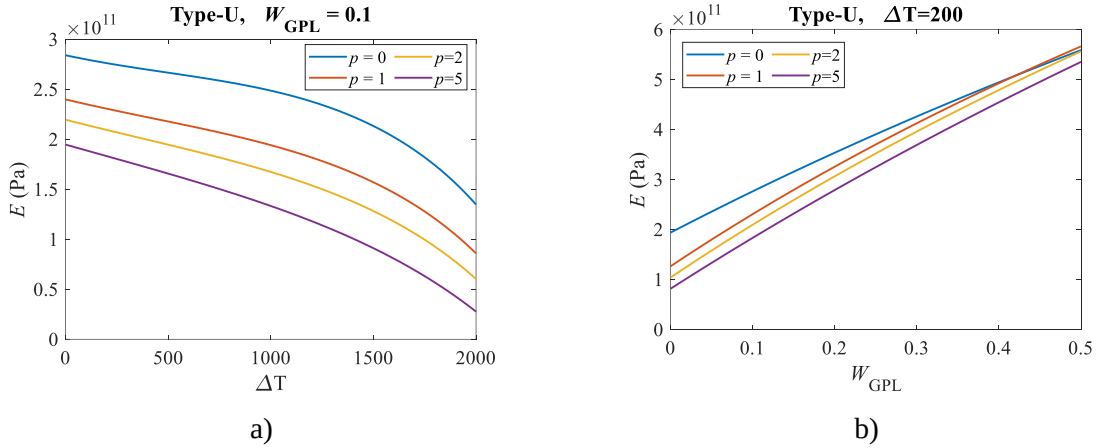

Figure 7. Variation of effective modulus of elasticity for extreme ΔT and W_{GPL} (ΔT ve W_{GPL} nin ekstrem değerleri için efektif elastisite modülünün değişimi)

A sensitivity analysis is carried out to examine how small changes in the ΔT, p and W_{GPL} parameters would impact the results. In the analysis, each parameter is increased by 10 % of the initial value for each step, finally reaching 50% above the initial value. As shown in Table 5, sensitivity analysis is carried out for E for mechanical properties and α for thermal properties. When the changes of the modulus of elasticity obtained for small changes in all three parameters are analyzed, it is seen that in the specified range, the lowest effect is ΔT with 0.1 %, while the highest effect is $W_{GPL}$with 20.47 %. Similarly, when the coefficient of thermal expansion is analyzed, the lowest effect is at ΔT with 0.44 %, while the highest effect is at W_{GPL} with 4.13 %

Table 5. Sensitivity analysis for small variations in fundamental parameters (Temel parametrelerdeki küçük değişimler için duyarlılık analizi)

	Parameters					
	ΔT=10	ΔT=11	ΔT=12	ΔT=13	ΔT=14	ΔT=15
E (GPa)	239.362	239.313	239.265	239.217	239.168	239.120
	W_{GPL}=0.1	W_{GPL}=0.11	W_{GPL}=0.12	W_{GPL}=0.13	W_{GPL}=0.14	W_{GPL}=0.15
E (GPa)	239.362	249.364	259.264	269.064	278.765	288.369
	p=1	p=1.1	p=1.2	p=1.3	p=1.4	p=1.5
E (GPa)	239.362	236.685	234.190	231.859	229.675	227.627
	ΔT=10	ΔT=11	ΔT=12	ΔT=13	ΔT=14	ΔT=15
α (K^{-1})(10^{-6})	10.654	10.664	10.673	10.682	10.691	10.701
	W_{GPL}=0.1	W_{GPL}=0.11	W_{GPL}=0.12	W_{GPL}=0.13	W_{GPL}=0.14	W_{GPL}=0.15
α (K^{-1})(10^{-6})	10.654	10.749	10.840	10.927	11.012	11.094
	p=1	p=1.1	p=1.2	p=1.3	p=1.4	p=1.5
α (K^{-1})(10^{-6})	10.654	10.735	10.808	10.874	10.934	10.990

4.CONCLUSIONS (SONUÇLAR)

In this research, the variation of effective mechanical and thermal material characteristics of double-FG GPLs-reinforced nanoplates with respect to temperature rise, GPL weight ratio and GPL dispersion patterns has been evaluated. According to the detailed parametric analysis, some important findings have been obtained. When the effects of temperature increase, GPLs weight ratio and GPLs dispersion patterns on the effective modulus of elasticity are examined, it is found that both temperature increase and increasing power law parameter significantly decrease the effective modulus of elasticity values. Additionally, it is discovered that the Young's modulus rise noticeably with rising GPL fraction and higher E values are obtained in the Type-X dispersion model. Examining the effective Poisson's ratio variation curves, it is concluded that the Poisson's ratio increases significantly with increasing temperature and power law parameter and decreases as GPL fraction rises. In addition, the Type-U dispersion model provides higher Poisson's ratio. The coefficient of thermal expansion of the proposed double-FG plate increases with ΔT and p in both Type-U and Type-X dispersion models. The effect of increasing GPL weight ratio on the thermal expansion coefficient tends to increase or decrease according to the power law index. Moreover, higher values of the thermal expansion coefficient are observed in the Type-U dispersion model. In the variation of the thermal conductivity coefficient, it is observed that the FG-plate shows more complex behavior. It is determined that the thermal conductivity coefficient of Si_3N_4, Ti-6Al-4V and GPL show different trends with increasing temperature, but the effective thermal conductivity coefficient of the plate tends to decrease due to the dominant thermal conductivity coefficient of GPL. Moreover, increasing power law index and GPL weight ratio increases the effective thermal conductivity coefficient of the plate. In addition, according to the sensitivity analysis performed with small changes in the determined parameters, W_{GPL} has the highest effect on the change in the modulus of elasticity, while ΔT has the least effect. Similarly, in the analysis for the coefficient of thermal expansion, it was determined that W_{GPL} has the highest effect and ΔT has the least effect. With this research, important results have been obtained on the determination of thermal and mechanical properties of double-FG GPL-reinforced nanoplates. These results are expected to contribute to the gap in the literature.

DECLARATION OF ETHICAL STANDARDS
(ETİK STANDARTLARIN BEYANI)

The author of this article declares that the materials and methods they use in their work do not require ethical committee approval and/or legal-specific permission.

Bu makalenin yazarı çalışmalarında kullandıkları materyal ve yöntemlerin etik kurul izni ve/veya yasal-özel bir izin gerektirmediğini beyan ederler.

AUTHORS' CONTRIBUTIONS (YAZARLARIN KATKILARI)

***Kerim Gökhan AKTAŞ*:** He constructed the mathematical model and the necessary codes for the analysis, performed the simulations, analyzed the results and wrote the manuscript.

Matematiksel modeli ve analiz için gerekli kodları oluşturmuş, simülasyonları yapmış, sonuçlarını analiz etmiş ve maklenin yazım işlemini gerçekleştirmiştir.

CONFLICT OF INTEREST (ÇIKAR ÇATIŞMASI)

There is no conflict of interest in this study.

Bu çalışmada herhangi bir çıkar çatışması yoktur.

REFERENCES (KAYNAKLAR)

[1] Saidi, H., Bouchafa, A., Tounsi, A., and Adda.Bedia, A. E.A., "Analysis of non-symmetric FG sandwich plates under Thermo-mechanical loading using a novel shear deformation theory with stretching effect," MATEC Web Conf., vol. 241, p. 1018, 2018.

[2] D. İpci and B. Yıldırım, "Free Vibration Analysis of a Functionally Graded Micro-Beam with Tapered Cross Section," Gazi Üniversitesi Fen Bilim. Derg. Part C Tasarım ve Teknol., vol. 9, no. 2, pp. 272–282, 2021.

[3] M. Arefi, "Buckling analysis of the functionally graded sandwich rectangular plates integrated with piezoelectric layers under bi-axial loads," J. Sandw. Struct. \& Mater., vol. 19, no. 6, pp. 712–735, 2017.

[4] R. Moradi-Dastjerdi and H. Malek-Mohammadi, "Biaxial buckling analysis of functionally graded nanocomposite sandwich plates reinforced by aggregated carbon nanotube using improved high-order theory," J. Sandw. Struct. \& Mater., vol. 19, no. 6, pp. 736–769, 2017.

[5] M. K. Apalak and M. D. Demirbas, "Thermal stress analysis of in-plane two-directional functionally graded plates subjected to in-plane edge heat fluxes," Proc. Inst. Mech. Eng. Part L J. Mater. Des. Appl., vol. 232, no. 8, pp. 693–716, 2018.

[6] C. T. Binh, T. H. Quoc, D. T. Huan, and H. T. Hien, "Vibration characteristics of rotating functionally graded porous beams reinforced by graphene platelets," J. Sci. Technol. Civ. Eng. - HUCE, vol. 15, no. 4, pp. 29–41, 2021.

[7] J. Yang, H. Wu, and S. Kitipornchai, "Buckling and postbuckling of functionally graded multilayer graphene platelet-reinforced composite beams," Compos. Struct., vol. 161, pp. 111–118, 2017.

[8] D. Chen, J. Yang, and S. Kitipornchai, "Nonlinear vibration and postbuckling of functionally graded graphene reinforced porous nanocomposite beams," Compos. Sci. Technol., vol. 142, pp. 235–245, 2017.

[9] S. Başkut and S. Turan, "Improving the Mechanical Properties of GPLs-SiAlON Composites by Microfluidization Technique as a New Approach to Dispersion of GPLs," Gazi Üniversitesi Fen Bilim. Derg. Part C Tasarım ve Teknol., vol. 10, no. 3, pp. 455–467, 2022.

[10] V. Kumar Dwivedi and D. Kumar, "Graphene as a stimulus for mechanical strength in glass-fiber reinforced polymers composite," World J. Eng., vol. 20, no. 1, pp. 143–149, 2023.

[11] Z. Li et al., "Uniform dispersion of graphene oxide in aluminum powder by direct electrostatic adsorption for fabrication of graphene/aluminum composites," Nanotechnology, vol. 25, no. 32, 2014.

[12] G. V Seretis, G. Kouzilos, A. K. Polyzou, D. E. Manolakos, and C. G. Provatidis, "Effect of Graphene Nanoplatelets Fillers on Mechanical Properties and Microstructure of Cast Aluminum Matrix Composites," Nano Hybrids Compos., vol. 15, pp. 26–35, 2017.

[13] K. Chu and C. Jia, "Enhanced strength in bulk graphene–copper composites," Phys. status solidi, vol. 211, no. 1, pp. 184–190, 2014.

[14] K. G. Aktaş, "3D wave dispersion analysis of graphene platelet-reinforced ultra-stiff double functionally graded nanocomposite sandwich plates with metamaterial honeycomb core layer," Mech. Time-Dependent Mater., vol. 28, no. 3, pp. 1873–1908, 2024.

[15] Z. Wu, A. E. Wilson-Heid, R. J. Griffiths, and E. S. Elton, "A review on experimentally observed mechanical and microstructural characteristics of interfaces in multi-material laser powder bed fusion," Front. Mech. Eng., vol. 9, no. July, pp. 1–20, 2023.

[16] M. Estili and Y. Sakka, "Dispersion and reinforcing mechanism of carbon nanotubes in a ceramic material," Funtai Oyobi Fummatsu Yakin/Journal Japan Soc. Powder Powder Metall., vol. 63, no. 11, pp. 955–964, 2016.

[17] M. Nouraei, V. Zamani, and Ö. Civalek, "Vibration of smart sandwich plate with an auxetic core and dual-FG nanocomposite layers integrated with piezoceramic actuators," Compos. Struct., vol. 315, p. 117014, 2023.

[18] H.-S. Shen, "Nonlinear bending of functionally graded carbon nanotube-reinforced composite plates in thermal environments," Compos. Struct., vol. 91, no. 1, pp. 9–19, 2009.

[19] S. Kamarian, M. Bodaghi, R. B. Isfahani, and J. Song, "Thermal buckling analysis of sandwich plates with soft core and CNT-Reinforced composite face sheets," J. Sandw. Struct. \& Mater., vol. 23, no. 8, pp. 3606–3644, 2021.

[20] P. Chen et al., "Preliminary analysis of a fully ceramic microencapsulated fuel thermal-mechanical performance," Mathematics, vol. 7, no. 5, p. 448, 2019, doi: 10.3390/math7050448.

[21] H. Le Ferrand, "Modeling the effect of microstructure on elastic wave propagation in platelet-reinforced composites and ceramics," Compos. Struct., vol. 224, p. 111105, 2019.

[22] W. Xiong, B. Blackman, J. P. Dear, and X. Wang, "The effect of composite orientation on the mechanical properties of hybrid joints strengthened by surfi-sculpt," Compos. Struct., vol. 134, pp. 587–592, 2015.

[23] C. García-Hernández et al., "Trochoidal milling path with variable feed. Application to the machining of a ti-6al-4v part," Mathematics, vol. 9, no. 21, p. 2701, 2021.

[24] S. R. Bakshi, V. Musaramthota, D. Lahiri, V. Singh, S. Seal, and A. Agarwal, "Spark plasma sintered tantalum carbide: Effect of pressure and nano-boron carbide addition on microstructure and mechanical properties," Mater. Sci. Eng. A, vol. 528, no. 3, pp. 1287–1295, 2011.

[25] O. A. Ogunmefun et al., "Densification, microstructure, and nanomechanical evaluation of pulsed electric sintered zirconia-silicon nitride reinforced Ti-6Al-4 V alloy," Int. J. Adv. Manuf. Technol., vol. 130, no. 7, pp. 3649–3660, 2024.

[26] W. Zhao, J. Cui, and P. Rao, "Effect of molten zone ablated by femtosecond lasers on fracture toughness of Si3N4 measured by SEVNB method," J. Eur. Ceram. Soc., vol. 38, no. 4, pp. 2243–2246, 2018.

[27] H. T. Thai and D. H. Choi, "A simple first-order shear deformation theory for the bending and free vibration analysis of functionally graded plates," Compos. Struct., vol. 101, pp. 332–340, 2013.

[28] H.-Q. Tran, V.-T. Vu, and M.-T. Tran, "Free vibration analysis of piezoelectric functionally graded porous plates with graphene platelets reinforcement by pb-2 Ritz method," Compos. Struct., vol. 305, p. 116535, 2023.

[29] M. Sobhy, M. A. Abazid, and F. H. H. Al Mukahal, "Electro-thermal buckling of FG graphene platelets-strengthened piezoelectric beams under humid conditions," Adv. Mech. Eng., vol. 14, no. 4, pp. 1–12, 2022.

[30] M. Sobhy and F. Alsaleh, "Nonlinear bending of FG metal/graphene sandwich microplates with metal foam core resting on nonlinear elastic foundations via a new plate theory," Mech. Based Des. Struct. Mach., vol. 52, no. 7, pp. 3842–3869, 2024.

[31] Y. S. Touloukian, Thermophysical properties of high temperature solid materials. New York: Macmillan, 1967.

[32] Touloukian YS, (1966) Thermophysical properties of high temperature solid materials. Volume 4. Oxides and their solutions and mixtures. Part 1, vol 1. New York: Macmillan, 1966.

[33] J. N. Reddy and C. D. Chin, "Thermomechanical analysis of functionally graded cylinders and plates," J. Therm. Stress., vol. 21, no. 6, pp. 593–626, 1998.

[34] D. G. Zhang, "Thermal post-buckling and nonlinear vibration analysis of FGM beams based on physical neutral surface and high order shear deformation theory," Meccanica, vol. 49, no. 2, pp. 283–293, 2014.

[35] L.-C. Tang et al., "The effect of graphene dispersion on the mechanical properties of graphene/epoxy composites," Carbon N. Y., vol. 60, pp. 16–27, 2013.

[36] F. Hua, W. Fu, Q. You, Q. Huang, F. Abad, and X. Zhou, "A refined spectral element model for wave propagation in multiscale hybrid epoxy/carbon fiber/graphene platelet composite shells," Aerosp. Sci. Technol., vol. 138, p. 108321, 2023.

[37] Y. W. Zhang, G. L. She, and M. A. Eltaher, "Nonlinear transient response of graphene platelets reinforced metal foams annular plate considering rotating motion and initial geometric imperfection," Aerosp. Sci. Technol., vol. 142, no. PB, p. 108693, 2023.

[38] M. Song, S. Kitipornchai, and J. Yang, "Free and forced vibrations of functionally graded polymer composite plates reinforced with graphene nanoplatelets," Compos. Struct., vol. 159, pp. 579–588, 2017.

[39] S. Qaderi, F. Ebrahimi, and V. Mahesh, "Free Vibration Analysis of Graphene Platelets–Reinforced Composites Plates in Thermal Environment Based on Higher-Order Shear Deformation Plate Theory," Int. J. Aeronaut. Sp. Sci., vol. 20, no. 4, pp. 902–912, 2019.

[40] M. A. Koç, İ. Esen, and M. Eroğlu, "Thermomechanical vibration response of nanoplates with magneto-electro-elastic face

layers and functionally graded porous core using nonlocal strain gradient elasticity," Mech. Adv. Mater. Struct., vol. 31, no. 18, pp. 4477–4509, 2024.